Transactions of the **13th International Conference on Structural Mechanics in Reactor Technology** (SMiRT 13), Escola de Engenharia - Universidade Federal do Rio Grande do Sul, Porto Alegre, Brazil, August 13-18, 1995

Ultimate inner pressure analysis on structural behavior of PCCV model including buttress and EAH

Hirade, T.[1], Hirose, M.[1], Naito, M.[1], Takumi, K.[1], Kimura, H.[2], Yokoyama, N.[2], Shimizu, F.[2]
1) Nuclear Power Engineering Corporation, Tokyo, Japan
2) Mitsubishi Research Institute, Tokyo, Japan

ABSTRACT

This paper shows a finite element method (FEM) analysis of ultimate structural behavior of a three dimensional (3-D) global model including buttresses and an equipment access hatch (EAH) on a pre-stressed concrete containment vessel (PCCV) specimen (Fig.1) subjected to internal over pressure. To a past experiment, the analysis result is compared with the experiment.

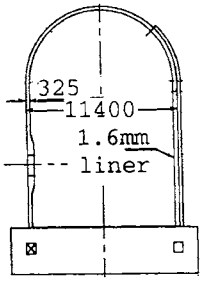

Fig.1. 1/4th scale PCCV specimen

ACKNOWLEDGEMENT

This work is performed under the auspices of the Ministry of International Trade and Industry, Japan.

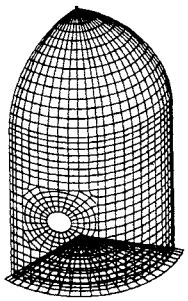

Fig.2. 3-D analysis model

1 OBJECTIVE

The objective in this analysis is to estimate an ultimate static response of an internally over pressurized PCCV including an EAH and buttresses (Fig.1).

2 ANALYSIS OBJECT

The analysis object (photo 1) is given by the unclosed information [1]~[9] where the specimen's basemat was swelled by an inner rubber bag pressurized hydrostatically and the whole specimen was tilted over to discontinue the loading. The basemat bar arrangement, etc. were not available, therefore we assume reasonable specifications.

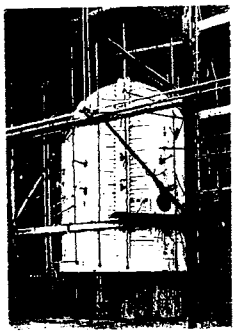

Photo 1. Analysis object [1]

3 THE ORIGINAL PCCV

The original PCCV has three buttresses, an EAH, and a 6mm thick steel inner liner (Fig.3). The 3.84m thick basemat has a pit named keyhole.

4 THE SPECIMEN

The 1/10th scale specimen has no steel liner (Fig.4). A 5.024m radius and 0.42m thick plane basemat dose not have keyhole nor tendon gallery. The rotational stiffness in the basemat-wall juncture corresponds to the stiffness of the original PCCV actual structure.

In the dome and barrel, basically, diameter deformed bars are arranged (Fig.5, Table 1), and in the barrel foot, the meridional rebar is formed by welding two more sizes of rebars.

8mm and 12.9mm diameter tendons are used in the ratio 2:1 in number respectively. Hairpin tendons have a vertical direction in the barrel. Their projected directions are 0° and 90° in the dome (Fig.6).

Hoop tendon length corresponds to two spans between the buttresses and overlaps in the length of one span. Dome hoop tendons are located from 0° to 30° in an angle of elevation [6].

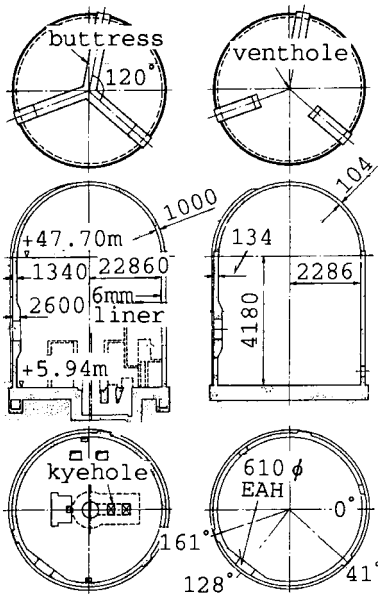

Fig.3. Actual PCCV [7]

Fig.4. Test specimen [7]

5 ANALYSIS MODEL

The analysis model is constructed using FEM general quadrilateral shell elements which have 4 nodes, a reduced Gaussian integration point, and 6 degrees of freedom.

5.1 MODELING RANGE

Fig.4 determines the geometrical whole shape of the analysis model which has cut off 120 degree range (Fig.2) of the entire structure. The analysis model has one third base slab, dome wall, and barrel wall including an EAH located at 128° between two half width buttresses at 41° and 161° in the cylindrical coordinate of the specimen.

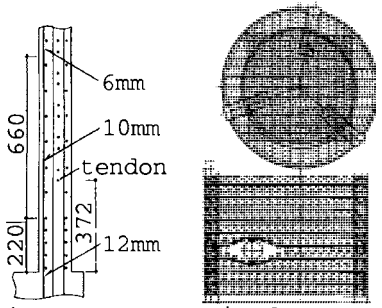

Fig.5. Bottom of the barrel [6]

Fig.6. An arrangement of tendon [2]

5.2 BARREL AND DOME

Fig.7 shows rebar shell element meshes in the general barrel and dome regions where the rebar arrangements are modeled by Fig.5 and Table 1. In the dome, the hairpin tendons are replaced meridionally, and the rebar and tendon ratios at the spring line are used even in the general region.

Table 1. Arrangement of the rebar and tendon in the barrel [6] and dome [2] (mm

		spacing		depth
		barrel	dome	
merid-ional	rebar	99.7(102)	99.7*(100*)	20(27)
	tendon	99.5	98.9*	-10***
hoop	rebar	104,52**	135	27(20)
	tendon	44	{44}	+10***

( ):outside,*:at the springline,**:in the f
***:based on the wall center,{ }:assumed va

5.3 BUTTRESS

Fig.8(a) shows the specimen's buttress and Fig.8(b) shows the analysis model where the same rebar spacing and shell reference frame are assumed as the barrel.

5.4 EQUIPMENT ACCESS HATCH

Around the EAH, the common shell reference frame is used (Fig.9(a).

The rebar and tendon are assumed to have r-θ directions (Fig.9(c,d)) with regard to the EAH center axis.

Here, the averaged values of the horizontal and vertical rebar and tendon ratios in the general barrel wall are assumed.

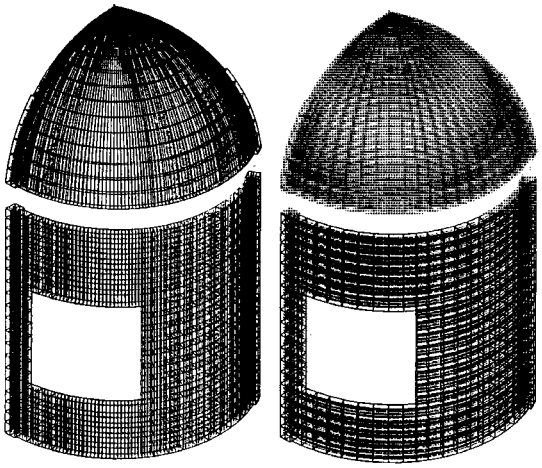

(a) meridional (b) hoop

Fig.7. Rebar shell element meshes

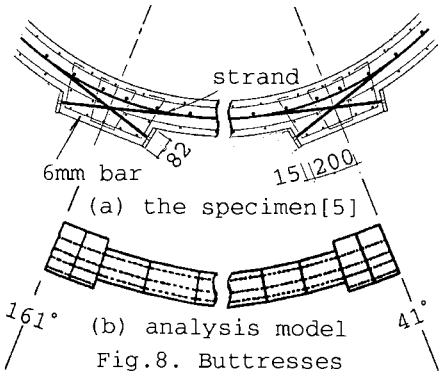

Fig.8. Buttresses

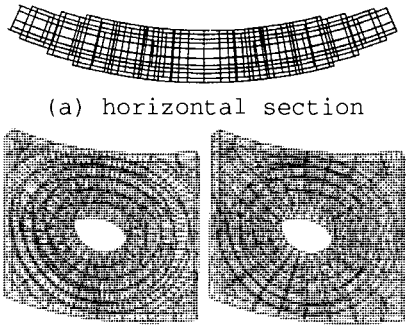

(a) horizontal section

(b) radial (c) circum-ferencial

Fig.9. Bar arrangement around the EAH

5.5 BASEMAT

The specimen's basemat section (Fig.10(a)) gives a few specifications in the analysis model (Fig.10(b),Fig.11). Regarding the unknown rebar ratio, applying a rebar ratio parametric study to an axisymmetric analysis, a reasonable bar arrangement is assumed based on the first yield pressure [6] of the radial bottom rebar in the experiment.
Table 2 shows the possible maximum rebar ratio where 2 basemat radial bars and 1 barrel tendon are arranged alternately.

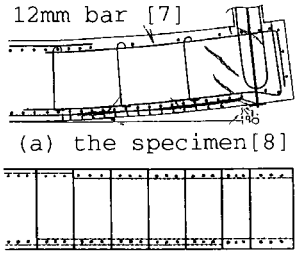

Fig.10. Section of the basemat

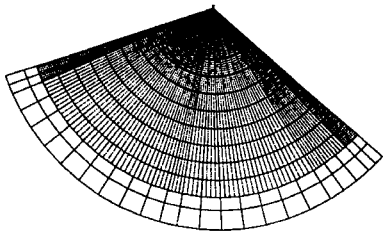

Fig.11. A radial rebar arrangement of the basemat (bottom, center)

Table 2. An assumption of the rebar arrangement in the basemat (case 5) (mm)

	position		range*	bar	space	depth
radi-al	top	center	0～1200	16mm	60	25
		end	1200～2512	12mm	48.5	57
	bot-tom	center	0～2000	16mm	60	25
		end	1000～2512	16mm	48.5	59
circum-feren-cial	top	center	0～1200	16mm	60	42
		end	1200～2512	16mm	240	42
	bottom		0～2512	16mm	60	42

*)modeling range in the radial direction

Table 3. Concrete material property [5]

	elastic modulus (MPa)	compressive strength (MPa)	tensile strength (MPa)	tensile cracking strain
wall	27000	43.2	4.3	0.00009
base	28000	44.8	4.5	0.00009

*) Poisson's ratio 1/6 is assumed

5.6 MATERIAL

Table 4. Rebar & tendon material property [5]

	dia-meter (mm)	area (mm2)	elastic modulus (MPa)
re-bar	6	27.77	191000
	10	77.45	190000
	12	112.61	203000
	16	198.22	-
ten-don	8	38	209200
	12.9	100	197400

*) Poisson's ratio 0.3

Table 5. Rebar & tendon stress strain data [5]

	stress (MPa)	elastic strain	plastic strain
6mm re-bar	324.1	0.0017	0.0000
	378.1	0.0020	0.0000
	433.9	0.0023	0.0001
	504.1	0.0026	0.0004
	603.2	0.0032	0.0028
	644.6	0.0034	0.0083
	764.0	0.0040	0.0977
10mm re-bar	258.2	0.0014	0.0000
	361.5	0.0019	0.0001
	439.0	0.0023	0.0003
	482.0	0.0025	0.0006
	524.2	0.0028	0.0012
	575.8	0.0030	0.0029
	604.3	0.0032	0.0082
	723.0	0.0048	0.0976
12,& 16mm re-bar	426.3	0.0021	0.0000
	461.8	0.0024	0.0001
	485.0	0.0030	0.0006
	583.0	0.1021	0.0992
8mm ten-don	1578.9	0.0075	0.0000
	1944.7	0.0079	0.0001
	1676.3	0.0080	0.0010
	1710.5	0.0082	0.0017
	1763.2	0.0084	0.0039
	1809.2	0.0086	0.0239
	1947.4	0.0093	0.0617
12.9 mm ten-don	1650.0	0.0084	0.0000
	1700.0	0.0086	0.0004
	1800.0	0.0091	0.0013
	1850.0	0.0094	0.0030
	1880.0	0.0095	0.0089
	1990.0	0.0101	0.0549

Table 3, 4, and 5 show a material property modeling. Perfect bond is assumed about tendons. After concrete cracking, the tension stiffening is defined by $-\sigma t/\varepsilon p$ where σt is a uniaxial maximum tensile strength of concrete and εp is a tension stiffening parameter.

6 ANALYSIS

Boundary condition is circumferential symmetry at 41° and 161° . In the wall-base juncture, not applying MPC, general barrel shell elements are filled up.

Dead load and water weight are neglected. Applying a general structure analysis code (ABAQUS Standard Ver. 5.3), 1300 and 1100MPa [6], and these average initial stresses are given to the meridional, hoop, and EAH region tendons respectively, then uniform static inner pressure is increased monotonically.

7 RESULT

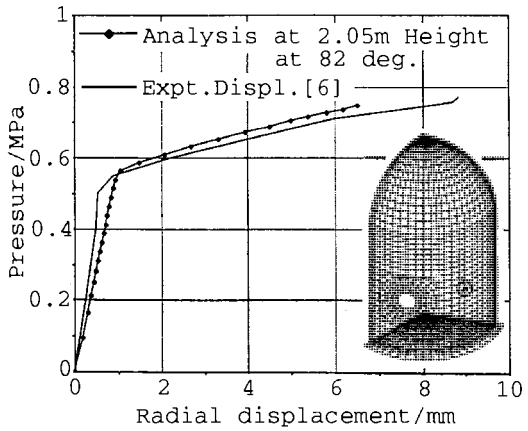

Fig.12. Barrel Wall Displacement

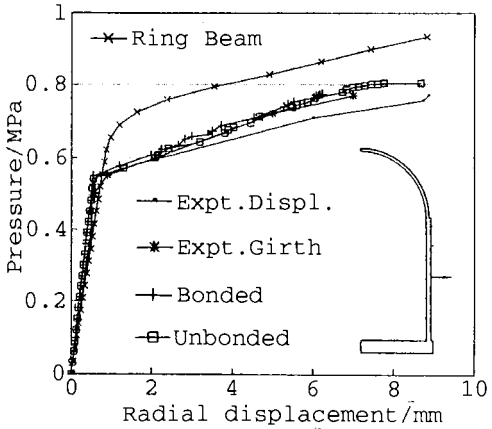

Fig.13. Barrel Wall Displacement at 2.2m Height [6]

Fig.12 shows a barrel wall displacement where our analysis indicates a good agreement with the experiment which is traced from Fig.13 [6]. In a tension stiffening parametric study, for εp=1.0E-3 and 3.0E-3, the calculations terminated at 0.52MPa and 0.55MPa respectively. Large εp values are not desirable but this 3-D global model is considered to have lower convergency than axisymmetric models.

Fig.14 shows a barrel wall deformation mode where the assumed specifications around EAH are considered to stiffen the deformation compared with the measured values (Fig.15 [5]), but the effect of buttresses is estimated.

Fig.16 shows a basemat uplift where the validity of our assumption is proved, compared with the experiment which is traced from Fig.17 [6] but a yielding phenomena is not simulated.

Fig.18 shows a basemat deformation mode where our analysis indicates a good agreement with the experiment which is traced from Fig.19 [6], but does not estimate a large rotation at the edge of the basemat. If an adhesion crack failure or a shear failure as Fig.10(a) [8] had occurred, FEM shell elements are not available.

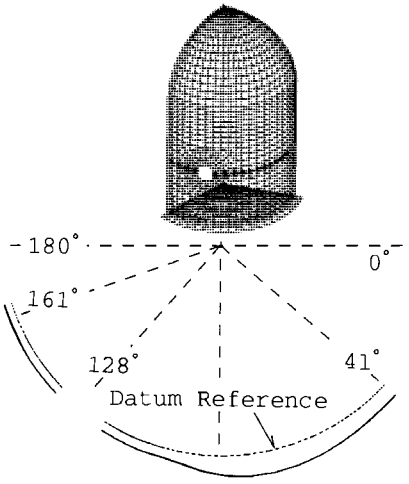

Fig.14. R-Theta Slice at Barrel Mid Height showing Displacement Analysis Results at 0.75 MPa (Displacements X 40)

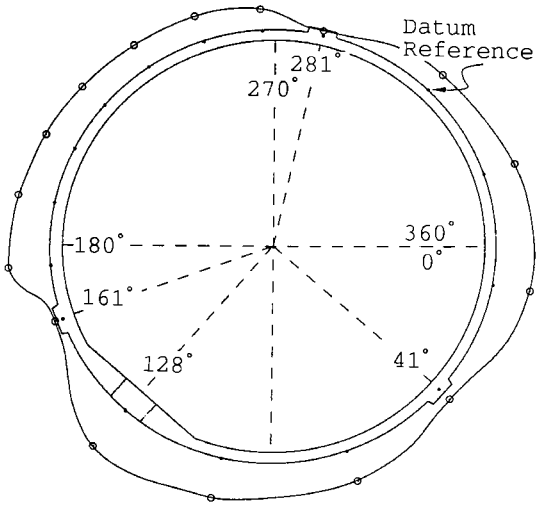

Fig.15. R-Theta Slice at Barrel Mid Height showing Displacement Transducer Readings at 112 psig (Displacements X 40) [5]

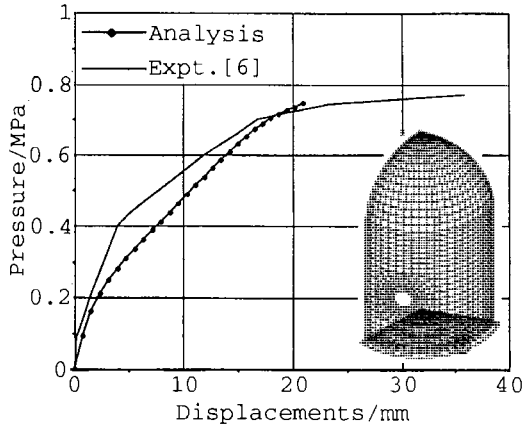

Fig.16. Basemat Uplift at 2.286m Radius

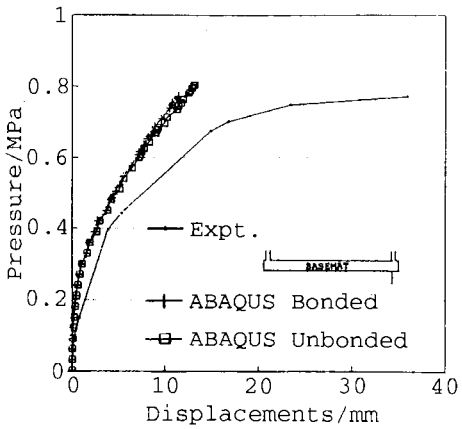

Fig.17. Basemat Uplift at 2.286m Radius[6]

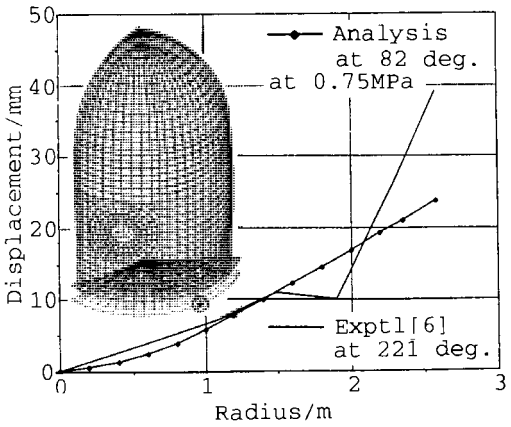

Fig.18. Basemat Uplift

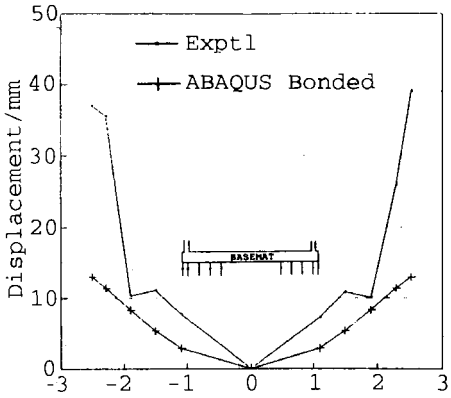

Fig.19. Basemat Uplift at 0.77MPa [6]

8 CONCLUSION

A FEM analysis is performed concerning an ultimate structural behavior of a 3-D global model including buttresses and an equipment access hatch of a past pre-stressed concrete containment vessel specimen subjected to internal over pressure. The analysis indicates some good agreements with the result in the experiment, therefore in this paper, the specimen's mechanical behavior in the experiment is generally estimated.

REFERENCES

[1] Lamas, C.(1988). "Proposal for a one tenth scale model test of the Sizewell 'B' containment," Proceedings of the Forth Workshop on Containment Integrity, 291-306, Arlington, Virginia.

[2] Smith, J.C.W. (1988). "The Design of a 1/10 Scale Model of the Sizewell B Primary Containment," Proceedings of the Forth Workshop on Containment Integrity, 307-324, Arlington, Virginia.

[3] Crowder, R.(1988). "New model for prestressed concrete containment test," Nuclear Engineering International, No.Suppl, 45-46.

[4] Varly, J.(1989). "Sizewell B model takes the pressure," Nuclear Engineering International, Vol.34, No.425, 58-59.

[5] Dameron, R.A.and Rashid, Y.R.(1990). "Sizewell-B 1:10 scale model pretest analyses and comparisons with experiment," ANATECH Report. submittal to Mr.Peter George, Nuclear Electric for inclusion in post test analyst's workshop proceedings.

[6] Wilkes, M.and Bleackley, M.H.(1990). "Finite Element Analysis of a 1/10 Scale Prestressed Concrete Reactor Containment To Overpressurisation," 2nd International Conference on Containment Design and Operation, Session 8, Toronto, Canada.

[7] Twindale, D.and Crowder, R.(1991). "Sizewell 'B' - a one tenth scale containment model test for the UK PWR programme," Nuclear Engineering and Design 125, 85-93.

[8] Dameron, R.A.and Rashid, Y.R.and Parks, M.B.(1991). " Comparison of Pre-Test Analyses with the Sizewell-B 1:10 Scale Prestressed Concrete Containment Test," Transactions of the 11th International Conference on Structural Mechanics in Reactor Technology (11th SMiRT), Volume H, 271-276, Tokyo, Japan.

[9] Palfrey, J.and Smith, J.C.W.(1991). "Ultimate Load Test of a 1/10 Scale Model Prestressed Concrete Containment," 11th SMiRT, Volume H, 277-282, Tokyo, Japan.